VNU Journal of Mathematics – Physics, Vol. 29, No. 3 (2013) 32-41

# The Microstructure of Amorphous Iron Nanoparticle

Mai Thi Lan*, Nguyen Van Hong, Nguyen Thu Nhan, Pham Khac Hung

*Department of Computational Physics, Hanoi University of Science and Technology*
*No. 1 Dai Co Viet, Hanoi, Viet Nam*

Received 26 August 2013
Revised 15 September 2013; Accepted 20 September 2013

**Abstract:** We have investigated the microstructure of amorphous iron nanoparticle (NP) and its bulk counterpart using molecular dynamic simulation with an embedded atom method (EAM). The NP models have a spherical shape and surface thickness of 3.6±0.125 Å. The microstructure of NP surface and core is analyzed through the coordination number distribution, density profile and distribution of simplex radius. Furthermore, the surface roughness has been identified via the distribution of distance from surface atom to NP surface. It was found that the microstructure of NP core is quite different from that of NP surface. However, their microstructure is almost independent on NP size. The simulation result shows that the NP as well as bulk counterpart contain a large number of "native vacancy". The glass transition temperature increases with NP size and depends on the fraction of surface atoms.

*Keywords:* structure, amorphous, nanoparticle, simulation, iron.

## 1. Introduction

Metal particles with nanometer size have attracted a great deal of interest because of a number of exciting potential applications in the biological fields, electronic and optical nanodevices [1,2]. With decreasing of the particle size to nanoscale, the particles are formed by a reduced number of atoms and a large fraction of them occupies the surface area. This process results in novel and different behavior which is determined not only by particle size, but also the intrinsic properties of the NP core as well as the NP surface [3,4]. Presumably, the peculiarity of NP is caused by the change in microstructure of core and surface particle during process of size reduction. Therefore, the understanding of NP core and surface at atomic level represents a great interest from both theoretical and practical viewpoints.

NP can be produced experimentally by several ways such as atomic deposition, mechanical milling, chemical methods or gas-aggregation techniques [3,4]. It was shown that the different sized particles can be created with well control experimental conditions. Although NP may be of different shape depending on the fabrication technique, but the spherical NPs are expected to be most stable

* Corresponding author. Tel.: 84-988277387
Email: lan.maithi@hust.edu.vn

form. Furthermore, the structure of NP with the same chemical composition may be much different, e.g. it may be crystaline, amorphous or composite. Compared to the bulk sample, the iron NPs show a great diversity in properties. It was revealed that both phases including ferromagnetic and paramagnetic occur in the iron NP and their properties depend significantly on the NP size. The structure of NPs was intensively studied using different techniques such as atomic force microscopy, transmission electron microscopy, extended X-ray absorption fine-structure techniques and simulation method [3-6]. The later could provide intrinsic information about the microstructure at atomic level. Nevertheless, very little works concerning with the microstructure of amorphous iron NP has been found yet. Therefore, it is worth to carry out a simulation of amorphous iron NP in order to compile a picture of its core and surface for NP with different size.

## 2. Calculation procedure

The molecular dynamic (MD) simulation was carried out in samples with spherical shape containing 1000, 2000, 3000, 4000 and 5000 atoms for NP and in simple cubic box with periodic boundary conditions for bulk. We use the Sutton-Chen EAM model which successful reproduces iron liquid at different temperatures and pressures [7].

We first replace $N$ atoms in a cubic box with periodic boundary condition for bulk or in a sphere with non-periodic boundary condition for NP. Then the melt equilibrated at 7000 K was obtained by relaxed the sample over $10^5$ MD steps under constant temperature and ambient pressure. The MD step is 1.4 fs. After that the melt is cool down to temperature of 300 K in order to construct the amorphous iron model. Next, final sample is obtained by relaxing the model for a long time (about $10^6$ MD steps).

## 3. Result and discussion

The first quantity we would like to discuss here is pair radial distribution function (PRDF) of amorphous iron at 300 K which is shown in Fig.1. Although there is some discrepancy around second peak between simulation and experimental data [8, 9], but in general they are in reasonable agreement which indicates a reality of constructed models. Compared to the bulk sample the PRDF of NPs almost coincides in the first and second peaks. The noticeable difference is found at distance $r$ bigger than 6.0 Å, the origin of which is ascribed to the surface part of NP, e.g. as the NP size increases, the contribution of surface to PRDF decreases. The snapshot of NPs is shown in Fig.2 and the main characteristics of obtained models are listed in Table 1. Here, to calculate the coordination number we used a fixed cutoff distance of 3.6 Å which is chosen as a minimum after the first peak of PRDF for the bulk model at 300 K. As shown from Table 1, the averaged energy per an atom as well as the mean coordination number of NP monotony changes with NP size. Due to the reduction of surface the contribution the value of $Z$ approaches to that of the bulk.

Fig.3 shows the distribution of coordination number for amorphous iron at 300 K. Largest difference observed here is the existence of two peaks located at about 9 and 13.2 for NP. Meanwhile,

there is only a pronounced peak for bulk. The height of those peaks also changes with NP size. Obviously, the origin of small peak is related to the surface contribution.

Table 1. The characteristics of amorphous iron models at 300 K; *E, $E_{core}$* and *$E_{surface}$* is averaged energy per atom for the system (bulk or NP), core and surface of NP, respectively; *Z, $Z_{core}$* and *$Z_{surface}$* is averaged coordination number for the system, core and surface of the NP, respectively*; $r_{core}$* is radius of core; *N, $N_{core}$* is number of atoms in the system and in the core, respectively

| System | *E, eV* | *$E_{core}$, eV* | *$E_{surface}$, eV* | *Z* | *$Z_{core}$* | *$Z_{surface}$* | *$N_{core}/N$* | *$r_{core}$*,Å |
|---|---|---|---|---|---|---|---|---|
| 1000 atoms | -2.1514 | -2.2853 | -1.9903 | 11.67 | 13.40 | 9.58 | 0.5460 | 12.04 |
| 2000 atoms | -2.1848 | -2.2908 | -2.0052 | 12.05 | 13.42 | 9.72 | 0.6290 | 15.96 |
| 3000 atoms | -2.1998 | -2.2880 | -2.0055 | 12.19 | 13.36 | 9.61 | 0.6880 | 18.93 |
| 4000 atoms | -2.2131 | -2.2976 | -2.0153 | 12.33 | 13.41 | 9.80 | 0.7008 | 20.92 |
| 5000 atoms | -2.2210 | -2.2953 | -2.0011 | 12.41 | 13.39 | 9.51 | 0.7472 | 23.01 |
| bulk | -2.3044 | - | - | 13.19 | - | - | 1.00 | - |

As seen certain NP characteristics are sensitive to the NP size due to the surface contribution. A question naturally raises is how to define the surface part of NP. Here we employ a method of sphere-shell. If the number of atoms belonging to spherical shell with thickness of 0.25 Å formed by two spheres with radius *r-0.125* and *r+0.125 Å* is determined, then one can infer two important quantities: the local density $\rho(r)$ and the local mean coordination number *Z(r)* on distance *r* from NP center. The profile of $\rho(r)$ and *Z(r)* is calculated from *r*=10 Å to $r_{max}$ with step of 0.25 Å. Here $r_{max}$ is maximal distance from all atoms to NP center. As shown in Fig. 4, function *Z(r)* slightly fluctuated around the value of 13.2 and then at some radius $r_{core}$ its value dropped to zero. In the case of $\rho(r)$ the amplitude of fluctuation is larger than that for *Z(r)*, but at the distance near $r_{core}$ the function also decreases towards zero. Such the radius $r_{core}$ can be determined from the functions *Z(r)* and $\rho(r)$. The radius $r_{core}$ is defined as the size of NP core, e.g. all atoms located in a sphere with radius $r_{core}$ belong to core and remaining atoms lie in the surface. The length $r_{max}$-$r_{core}$ is corresponded to the thickness of surface which is found to be 3.6 ±0.125 Å.

Table 2. The characteristics of NP surface roughness

| System | 1000 | 2000 | 3000 | 4000 | 5000 |
|---|---|---|---|---|---|
| Mean, Å | 1.70 | 1.67 | 1.49 | 1.64 | 1.35 |
| Variance, $Å^2$ | 0.35 | 0.37 | 0.58 | 0.39 | 0.38 |

Further relevant information about NP is the surface roughness which is determined by mean of the distribution of the distance from surface atom to the NP surface: $r_{is}$-$r_{core}$ (DD). Here $r_{is}$ is a distance from $i^{th}$ surface atom to the center of NP. For small NP the DD has not well defined form, but with increasing NP size there is a pronounced peak located in the interval of 1.3-1.8 Å. In addition, the form of DD for large NP is well defined and similar to each other (see Fig.5). The mean and variance of quantities $r_{is}$-$r_{core}$ are listed in Table 2. It can be seen that there is not well defined trend with NP

size. Presumably, the surface roughness of NP is defined not only by $r_{core}$, but by both parameters: the faction of surface atoms $N_{surface}/N$ and size of NP core $r_{core}$. Note that the number of atoms in surface $N_{surface} = N - N_{core}$ may be different for different NP with the same $r_{core}$. Now we turn on to discuss the surface and core microstructure. As shown in Table 1 the averaged energy per an atom in core is changed slightly with NP size and approached to the value of bulk. Similar trend is observed for the mean coordination number, although the fraction of core atoms and radius of core significantly changes. Furthermore, the value of both quantities $E_X$ and $Z_X$ ($X$ indicates the surface or core) is quite different for core and surface. For instance, the $Z_{core}$ and $Z_{surface}$ of sample with 3000 atoms are 13.36 and 9.61, respectively. To infer more information we determine the coordination number distribution for core (CNDC) and surface (CNDS). Fig.6 shows that the CNDCs as well as CNDS for different NPs are very similar to each other. The CNDC has a pronounced peak at 13.4, meanwhile, for the CNDS one can see a peak at 9.0. Unlike CNDC the CNDS has an ansymmetrical form. Therefore, the microstructure of core seems to like that of the bulk and changes slightly with NP size. As regarding to surface, its microstructure is almost independent on NP size. Useful information about local structure can be inferred from simplex analysis. The simplex is defined as a set of four nearest neighboring atoms which form a tetrahedron. In addition, there is not any atom inside the circum-sphere (CS) of this tetrahedron (the vertices of the tetrahedron lie on surface of CS). The simplex radius is denoted to the radius of CS. More detail about the method determining the simplexes can be found elsewhere [6]. Fig.7 shows the distribution of simplex radius (DSR) for amorphous iron. In the case of surface we consider only simplex with distance between its CS and NP center is less than $r_{max}$. For bulk case the DSR is widely spread in the interval from 1.4 to 2.55 Å. It is worth to note that the shortest distance between two atoms in the bulk is 2.05 Å. Therefore, if one inserts an atom inside the simplex with radius bigger than 2.05 Å, then the distance between the inserting atom and any another atom is also bigger than 2.05 Å. It means that such simplex likes an "empty node" in amorphous matrix, where one atom is removed. This picture is similar to the case that if we remove one atom from the crystal lattice, for instance bcc iron, then a large simplex is created. The distance from this simplex to any atom is bigger than shortest distance between two atoms in the bcc lattice. This simplex is considered as vacancy in bcc lattice. By analogy the simplex with radius bigger than 2.05 Å, can be considered as a “native vacancy” in amorphous iron. Schematic illustration for determining the native vacancy in amorphous matrix is shown in Fig.8. The native vacancy could play a role of vacancy but their concentration weakly depends on the temperature. This leads to that the activation energy for iron self-diffusion is mainly determined by migration part and not as sum of migration and formation energy. This property is observed experimentally for certain amorphous Fe-based alloys where the activation energy is significantly lower than ones of the crystalline counterpart [10]. As seen from Fig.7 the DSR for different NPs is also similar to each other indicating again their similar microstructure. It is interesting to determine the number of non-overlapping simplexes with radii bigger than 2.05 Å which determines the concentration of native vacancies. The result is presented in Table 3. It can be seen that the number $N_{vac}$ monotoneously decreases with increasing the size of NP. Compared to the core, the number $N_{vac}$ in surface is much larger. Although the number of native vacancy has a little influences on the main characteristics such as $E_x$, $Z_x$ and the distribution of coordination number,

however it characterizes a homogeneity in amorphous structure. Therefore, the bigger the NP size is, the more homogeneous is its structure. Combining with above result one can conclude that the diversity in NP properties is caused mainly by the difference of the core radius $r_{core}$ and the fraction of surface atoms $N_{surface}/N$.

Table 3. The number of native vacancy per atom, $N_{vac}$.

| System | 1000 | 2000 | 3000 | 4000 | 5000 | Bulk |
|---|---|---|---|---|---|---|
| $N_{vac}$ | 0.054 | 0.020 | 0.010 | 0.008 | 0.004 | 0.001 |

Amorphous material transforms from glass solid form to liquid-state at glass transition temperature $T_g$. For MD simulation the temperature $T_g$ can be determined via the intersection of a linear high temperature and low temperature extrapolation of the potential energy of the system as shown in Fig.9 for the NPs with 1000 and 5000 atoms. In order to evaluate the size effect of NP we determine the $T_g$ for different NPs. The estimate of $T_g$ was equal to 860, 872, 928, 944 and 960 K for NP samples with 1000, 2000, 3000, 4000 and 5000 atoms, respectively. The glass transition temperature for bulk liquid obtained in present work is around 1050K which is higher than that for NP. This is in agreement with values experimentally observed for organic NP. Although fundamentally important, the nature of glass transition is not well understood [11]. Several parameters which influence on glass transition in system at nanoscale can be considered such as the size effect, interfacial effect, macroscopic confinement effect and boundary conditions [12]. In accordance to our simulation, the variation of temperature $T_g$ with NP size is ascribed to the fraction of core atoms $N_{core}/N$.

## 4. Conclusion

In summary we employ molecular dynamic simulation with Sutton-Chen EAM to investigate the microstructure of amorphous iron NP and its bulk counterpart. Our study addresses the microstructure of the NP core with different size and the surface with thickness of 3.6 ±0.125 Å. The result shows that the structural and energetic characteristics of NP core such as the mean potential energy per an atom, statistic of the coordination number and simplexes are almost independent on NP size. The same trend was found for NP surface indicating that their microstructure is little changed with NP size. Compared to bulk counterpart we observe the similarity of the microstructure with NP core. Therefore, the great diversity in properties of NP is related to the fraction of surface atoms and size of core. Our simulation shows that the NP as well as bulk contains a number of "native vacancy" which is a simplex with radius bigger than 2.05 Å. The concentration of native vacancy monotony decreases with increasing the NP size. The glass transition temperature is determined via intersection of a linear high temperature and low temperature extrapolation of potential energy of system. It was found that the glass transition temperature increases with NP size and is lower than that of bulk counterpart.

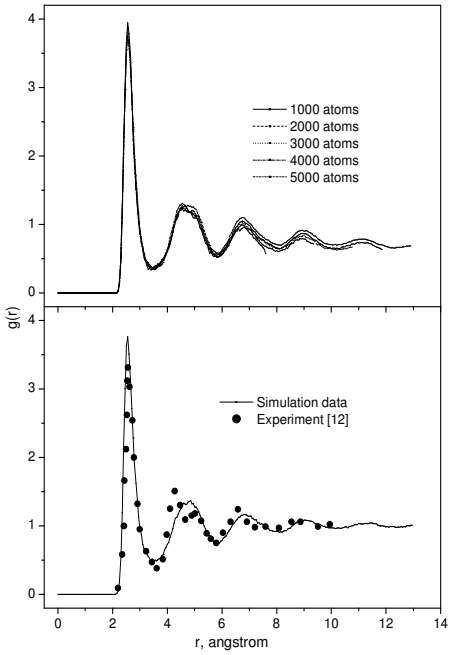


Fig. 1. The pair radial distribution functions for NP sample (top) and bulk (bottom) at 300 K.

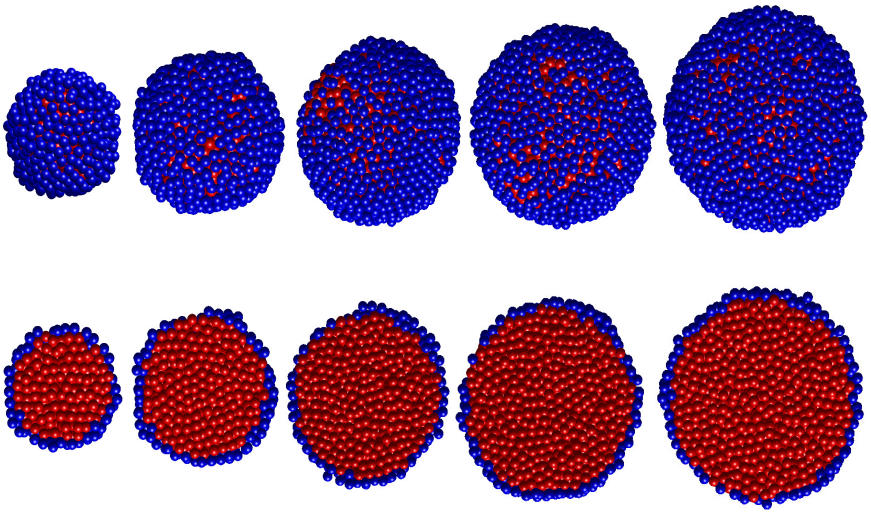

Fig. 2. The snapshot of NP (top) and half of NP (bottom) which consist only of atoms *i* with coordinate $y_i < 0$ (another half of NP with coordinate $y_i > 0$ has been removed); The blue (black in print version) and red (gray in print version) spheres represent the surface and core atom, respectively.

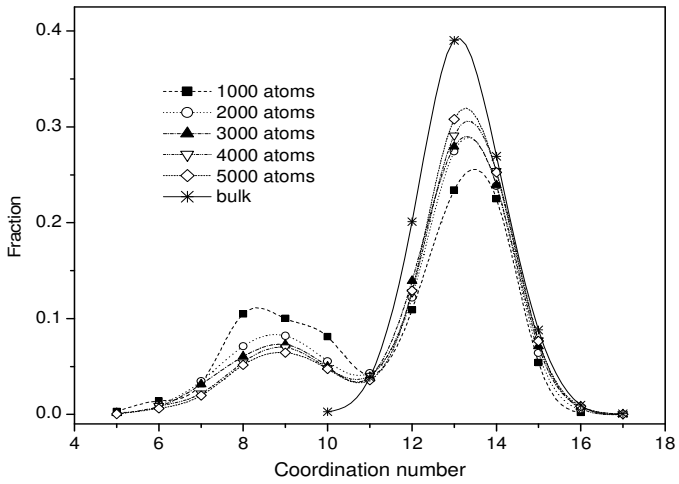


Fig. 3. The coordination number distribution in amorphous iron at 300 K.

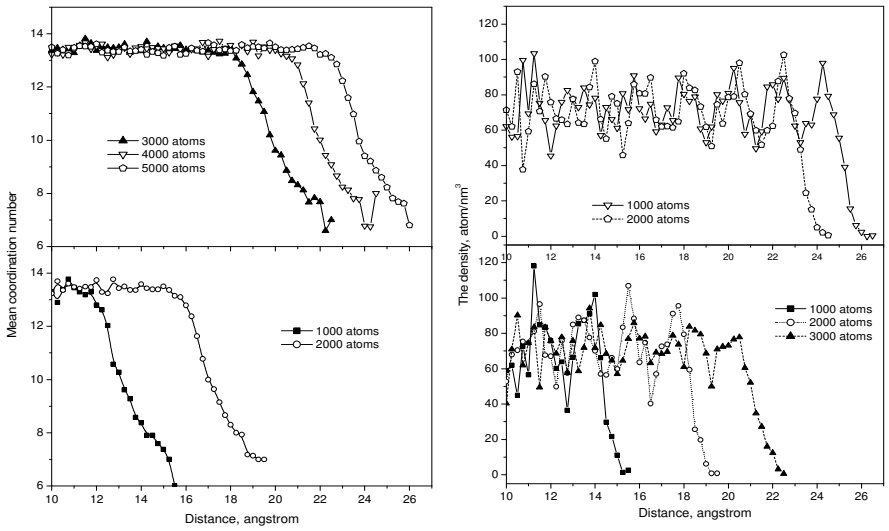


Fig. 4. The local mean coordination number (left) and local density (right) distributions for spherical shell.

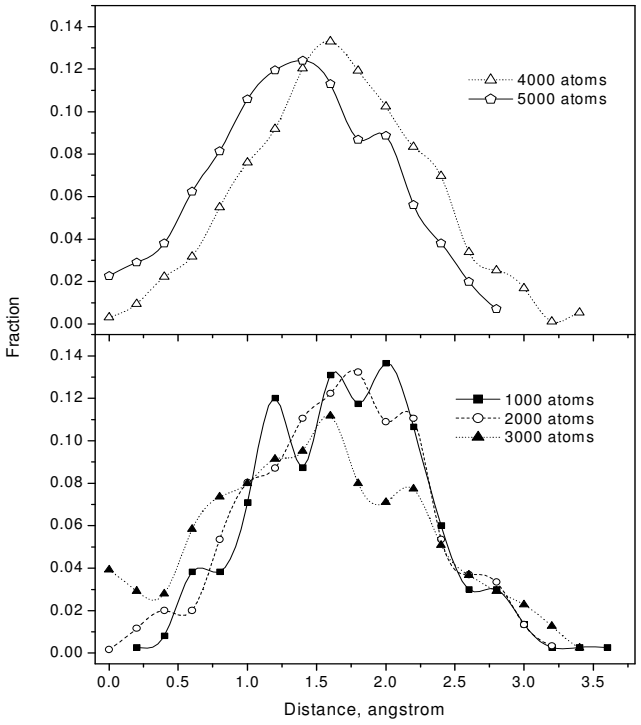


Fig. 5. The distribution of distance $r_{is}$-$r_{core}$ for amorphous iron NP.

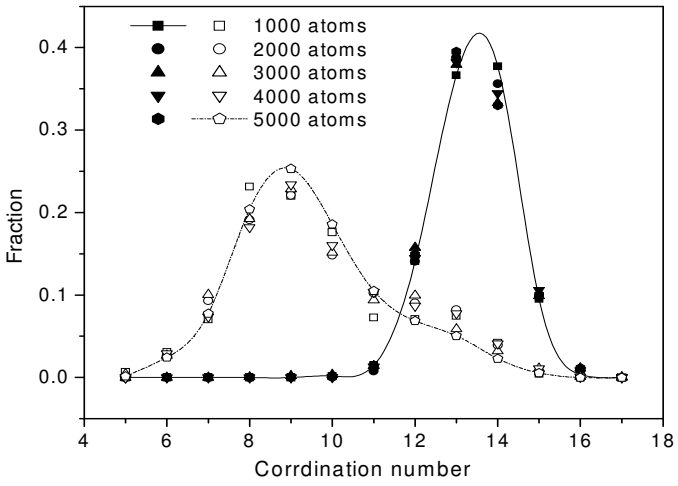


Fig. 6. Coordination number distribution; filled and unfilled symbols represent the core and surface case, respectively.

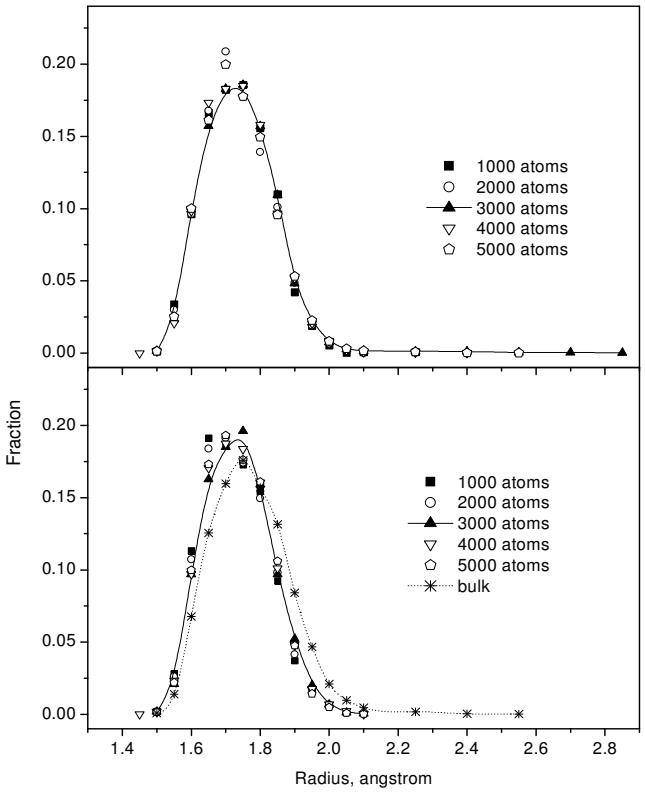


Fig. 7. The distribution of simplex radius for surface (top) and core (bottom).

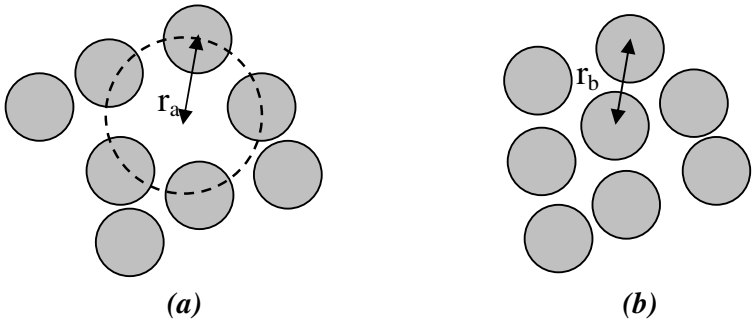


Fig. 8. Schematic illustration of "vacancy native", here filled circles are denoted to atoms. There are two locations (*a)* and (*b)*. At first one a simplex (native vacancy) has a distance $r_a$ bigger than $r_b$, where $r_b$ is a shortest distance between two atoms in the location (*b)*.

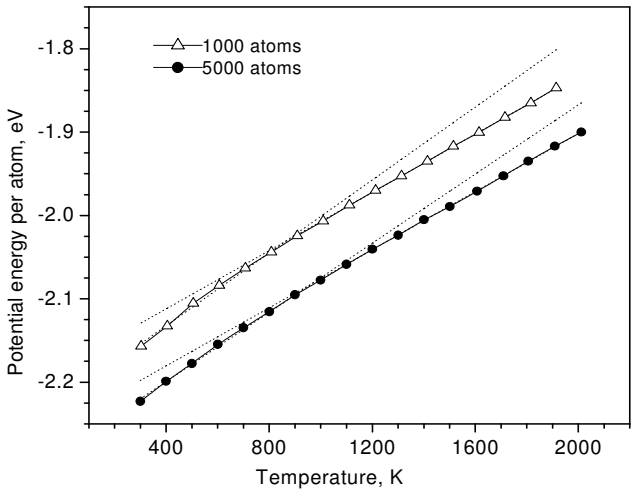


Fig. 9. Determination of glass transition temperature of NP with 1000 and 5000 atoms.

**Acknowledgement**

The authors are grateful for support by the NAFOSTED Vietnam (grant *No **103.01-2011.32***).

**References**

[1] J. Zhang, K. Sasaki, E. Sutter, R.R. Adzic, Science, 315 (2007), 220.
[2] P. Tartaj et al 2003 J. Phys. D: Appl. Phys. 36 (2003), R182.
[3] J. Carvell, E. Ayieta, A. Gavrin, Ruihua Cheng, V. R. Shah, P. Sokol. J. Appl. Phys. 107 (2010), 103913D.
[4] G. Kataby,A. Ulman, R. Prozorov,A. Gedanken, Langmuir , 14 (1998), 1512.
[5] B.T.H.L. Khanh, V.V. Hoang and H. Zung,Eur. Phys. J. D, 49 (2008), 325.
[6] P.K.Hung, P.H.Kien, Eur. Phys. J. B 78 (2010), 119.
[7] L. Koči, A. B. Belonoshko, R. Ahuja, Phys. Rev. B 73 (2006), 224113.
[8] Ichikawa, Phys. Status Solidi (a) 19 (1973), 707.
[9] Y. Waseda, H.S. Chen, Solid State Commun. 27 (1978), 809.
[10] W. Frank, A. Horner, P. Scharwaechter and H. Kronmiiller, Materials Science and Engineering, A 179/A 180 (1994), 36.
[11] C. A. Angel, K. L. Ngai, G. B. McKenna, P. F. McMillan, S. W. Martin, J.Appl. Phys., 88, 6 (2000), 3113.
[12] Alcoutlabi M. and McKenna G. B ., J. Phys.: Condens.Matter 17 (2005), 461